

# Indoor Positioning System based on Sensor Fusion for the Blind and Visually Impaired

Thomas Gallagher, Elyse Wise, Binghao Li, Andrew G. Dempster, Chris Rizos  
School of Surveying and Geospatial Engineering, UNSW  
Sydney, Australia  
t.gallagher@unsw.edu.au

Euan Ramsey-Stewart  
Ramsey Stewart Industrial Design  
Sydney, Australia  
euan@rsid.com.au

**Abstract**— There are over 1.2 million Australians registered as having vision impairment. In most cases, vision impairment severely affects the mobility and orientation of the person, resulting in loss of independence and feelings of isolation. GPS technology and its applications have now become omnipresent and are used daily to improve and facilitate the lives of many. Although a number of products specifically designed for the Blind and Vision Impaired (BVI) and relying on GPS technology have been launched, this domain is still a niche and ongoing R&D is needed to bring all the benefits of GPS in terms of information and mobility to the BVI. The limitations of GPS indoors and in urban canyons have led to the development of new systems and signals that bridge the gap and provide positioning in those environments. Although still in their infancy, there is no doubt indoor positioning technologies will one day become as pervasive as GPS. It is therefore important to design those technologies with the BVI in mind, to make them accessible from scratch. This paper will present an indoor positioning system that has been designed in that way, examining the requirements of the BVI in terms of accuracy, reliability and interface design. The system runs locally on a mid-range smartphone and relies at its core on a Kalman filter that fuses the information of all the sensors available on the phone (Wi-Fi chipset, accelerometers and magnetic field sensor). Each part of the system is tested separately as well as the final solution quality.

*Kalman filter; sensor fusion; indoor positioning and navigation; blind and visually impaired; user centred design*

## I. INTRODUCTION

Smartphones in general and the applications that leverage their hardware have revolutionized the way we interact with our environment and each other. They are a formidable tool to help us better communicate, learn new skills, navigate and interact with our surroundings. How often can one get lost nowadays when the entire world map and a relatively accurate position are available in the palm of one's hand within seconds? This miracle of the modern world has largely been made possible by the launch and maintenance of the Global Positioning System (GPS) by the US government, and more recently by efforts by other countries to deploy their own Global Navigation Satellite System (GNSS). GNSS receiver chips are now near ubiquitous, present in our cars, phones, cameras etc. However, it is well known that GNSS systems are not perfect as they rely on faint radio signals that can be blocked or reflected by man-made structures, resulting in a severe degradation of accuracy or in a complete loss of

availability. In the recent years, new ways of positioning people or assets indoors have been developed that aim to "bridge the positioning gap" that are now trickling down to the mass market; see for instance the launch of Google Indoor Maps for all Android smartphones [1].

The Blind and Visually Impaired (BVI) are a community that can benefit immensely from these new technologies as navigation and orientation is one of the main challenges they are faced with. Among the BVI, smartphones are being adopted more and more by people who recognize the potential of these devices. Although a number of products specifically designed for the BVI have been launched, the domain is still a niche and ongoing R&D is needed to bring all the benefits of indoor and outdoor positioning in terms of information and mobility to the BVI. In the case of indoor positioning technologies which are still in early stages, it is therefore crucial to design with the BVI in mind, to make them accessible from scratch. With the immense potential of these new technologies in terms of mobility and information, the BVI cannot be put aside and be an afterthought of designers.

In this paper, we will therefore present an indoor positioning system designed in that way. An important part of this paper examines the user requirements of the BVI, including accuracy, reliability and interface design. The data from this part comes from a pilot survey run by the authors among approximately 25 BVI persons, and that focused on location based information, navigation, mobility, and experiences with current smartphone products for the BVI. We then present the system which runs locally on a mid-range smartphone and that relies at its core on a Kalman filter that fuses the information output by all the sensors available on the phone. The third part of the paper tests each of the system parts individually as well as the final solution quality.

## II. SYSTEM DESIGN

### A. User Requirements

In this part, we will examine the user requirements that need to be taken into account when designing a navigation solution for the BVI. In order to assess these requirements, we ran a phone survey campaign amongst BVI people in Australia. More details about the output of this ongoing campaign will be published in the future and what follows is an early summary of our discussion with the participants, as well as our own

input. A full paper dealing with user requirements for a positioning system for the BVI can be found in [2].

First, it is important to make the distinction between mobility and navigation challenges, as well as between primary and secondary aids, as presented in [3]. The challenge of mobility is to identify a safe path that avoids obstacles and hazards by detecting stationary and mobile objects that can be dangerous for the person. Primary aids aim at solving this challenge, and can, at least in theory, safely be used alone. Examples of primary aids include the widely used long cane and guide dog, or systems such as the UltraCane or BAT “K” Sonar Cane [4] which detect obstacles using ultrasound. The challenge of navigation is that of knowing your current location, what is around you and how to get to a destination. Secondary aids that aim at solving this challenge cannot be used by themselves and are meant to augment primary aids. Examples of available secondary aids include the Miniguide [3] or the TrekkerBreeze [5]. Our system can be classified as a secondary aid as it is not designed to be used by itself and will not provide detailed obstacle avoidance features. Rather, it will provide “accessible signage”, which is what the BVI lack most, according to our survey. In terms of obstacle avoidance, the long cane, its technological extensions and guide dogs (when available) already are state of the art solutions that are immensely useful to the BVI. As a consequence, the system doesn’t need to provide centimetre accuracy; high level navigation can be provided with a few meters accuracy.

One common issue of all positioning methods is exceptional degradation of accuracy or complete failure of the positioning engine. Depending on the application of the positioning system, it is more or less critical to be able to detect those events. In the case of a commercial air pilot using GNSS for a high precision approach, one can easily understand the need to make sure that the aircraft’s position is both accurate and robust. The same level of reliability must be reached when designing a navigation solution for the blind for health and safety reasons (stairways, for instance, are particularly dangerous areas). If the robustness of the positioning engine cannot be guaranteed, the user interface must be designed so that the user knows that he/she cannot put all his/her trust in the software and must remain vigilant. This can be done either by the positioning system reporting an error estimation (GPS for instance has a Dilution of Precision (DOP) value), or by the system designer guaranteeing a probability distribution for the accuracy of the position. Another aspect of reliability is the range of the system in terms of battery life. As the software relies on continuous polling of sensors that consume a high level of power, the battery level must be monitored to avoid a loss of navigation in a dangerous area, putting the user at risk.

The user interface must also be designed in such a way so as not to overload the senses. The BVI use all the senses other than sight (smell, sound and touch) to navigate and mentally reconstruct the environment. As a consequence, the interface must be as light as possible on these senses, while still providing the user with useful and meaningful information. That implies knowing what type of information is needed and how often and when it should be delivered to the user. This information will be derived fully from the answers of participants to our survey and published in a future paper.

Another consequence is that the user cannot be required to carry the device in his or her hand. Indeed, the user will often use a long cane, guide dog or other means of primary navigation aid, leaving only one hand free for other actions, safety when falling for instance. The navigation device must therefore work independently of its orientation and position on body.

Most of the survey participants also emphasized the aesthetics and portability requirements, stating that the device should be unobtrusive, inconspicuous and easy to carry. Most past navigation solutions for the BVI are bulky and need several external sensors fixed on the body to operate. Although interesting from a research point of view, such devices will never be adopted by the BVI as they feel alienated and put apart from others when using them. Moreover, the device should not be visibly expensive high technology for safety reasons.

### B. Overview of the System

An initial vision for the system has been presented in [6]. For all the reasons stated in the section above, we decided to choose a smartphone as a platform rather than a custom design. First, all modern smartphones have all the sensors required to provide indoor and outdoor positioning and navigation: A-GPS and Wi-Fi chip, accelerometer, gyroscope and magnetic flux sensor. Some recent smartphones also incorporate a barometer for altitude determination. Smartphones are also near ubiquitous so that they do not attract attention from other people. Early results from our survey campaign also indicate that more and more BVI own a smartphone and are familiar with how to operate it. In that way, they will not be required to acquire an extra piece of equipment and learn how to use it. Moreover, smartphones can also be placed anywhere on the body or in a backpack, leaving the user’s hands free.

To provide indoor positioning, our system fuses information provided by all the smartphones sensors (Wi-Fi, accelerometer and magnetic flux sensor) except for the gyroscope which will be integrated at a later stage. We chose the Android operating system as it provides all the APIs necessary to access all the sensor data. The smartphone used is a Samsung Nexus S, which contains all the sensors required and has a short Wi-Fi scan rate (roughly 0.7s).

### C. Kalman filter

A Kalman filter was chosen to fuse the data coming from all sensors. It has been proven to be an appropriate tool for multi-sensor positioning systems and is widely used for outdoor integrated navigation, combining GPS and INS measurements as presented in [7] and [8]. Moreover, it is computationally efficient and can be easily implemented on current smartphones. Fig. 1 illustrates the overall structure of the filter. The two main phases of the filter are prediction and update. In the prediction stage, the motion model is used to predict where the user should be at  $t+1$ . The motion estimator uses the accelerometer and magnetic sensor to compute a speed and heading value. In the update stage, the positions obtained through the Wi-Fi positioning engine are used to correct the predicted position.

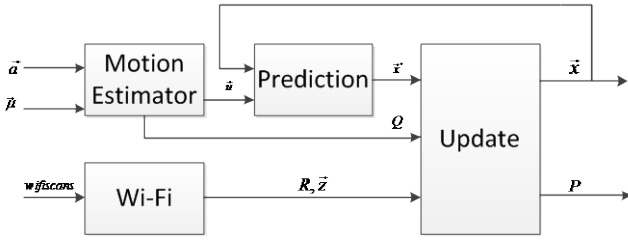


Figure 1. Kalman filter overall architecture

The state vector that is estimated is as following:

$$\vec{x} = [x, y]^T$$

where  $x$  and  $y$  are the local coordinates of the user on the floor plan. The prediction equation, which predicts where the user should be at  $t+1$  based on inertial sensor information, is

$$\vec{x}_{k+1} = \vec{x}_k + \begin{bmatrix} \Delta t \cdot v_k \cdot \cos(\theta_k) \\ \Delta t \cdot v_k \cdot \sin(\theta_k) \end{bmatrix}$$

where

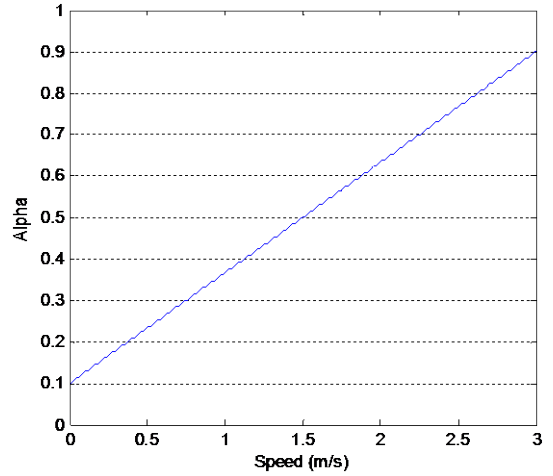
$$\theta_{k+1} = \alpha \cdot \theta_k + (1 - \alpha) \cdot \theta_c$$

Here,  $\theta_k$  is the estimated user heading relative to true north at time  $t$ ,  $\theta_c$  is the heading value provided by the magnetic compass and  $v_k$  is the speed of the user at time  $t$ . The main issue with the compass indoors is that it is heavily influenced by metal structures or objects present in the building. For this reason, the raw heading values output from the compass cannot be used as is and need smoothing. This is realised with the smoothing parameter  $\alpha$  which is a real number between 0 and 1 which depends on the estimated speed of the user  $v_k$ . Indeed, when a user is walking fast, he or she is less likely to make big changes in direction. But when the user is standing still, that is when he or she is more likely to turn around. Fig. 2 illustrates how the parameter  $\alpha$  evolves with speed. It is a very basic model but more complex models can be built by taking into account other sensors, especially a gyroscope as presented in [8] and [9].

The measurements used in the update stage of the filter are the positions calculated by the Wi-Fi fingerprinting engine:

$$\vec{z} = [x, y]^T$$

The most difficult task when implementing a Kalman filter is to get a good estimate of the noise covariance matrixes  $Q_k$  and  $R_k$ . Typically, the process noise covariance matrix  $Q_k$  should be updated based on the current speed and heading estimated errors. However, these errors are difficult to model and an empirically chosen constant matrix  $Q$  was chosen. The


 Figure 2. Evolution of  $\alpha$  with speed

covariance matrix of the observation noise  $R_k$  is defined as follows

$$\begin{cases} \vec{z}_k = H_k \vec{x}_k + \vec{v}_k \\ \vec{v}_k \sim N(0, R_k) \end{cases} \quad (1.1)$$

Here, the measurements are positions obtained by using a Wi-Fi fingerprinting method. Unlike GPS where most receivers supply parameters such as the Dilution of Precision (DOP), there are very few metrics to estimate the error of positions calculated with fingerprinting. Some examples can be found in [10], [11], or [12], but this is still an early research area. Thus, as with the  $Q$  matrix, we chose an empirical constant matrix  $R$  to model the observation noise. Details on how the  $Q$  and  $R$  matrixes were chosen are given in part II section E. It is clear however that further investigation is needed to obtain a better estimate of these matrices as they are critical to the operation of the filter.

#### D. Wi-Fi measurement model

The Wi-Fi positioning engine that feeds the Kalman filter is based on the now common fingerprinting technique which was first introduced by [13], and used in [14] for instance. This technique has two main phases. The first phase, called the training phase, consists in building a database of Wi-Fi fingerprints which associate each location with a unique set of access points (APs) and signal strengths. The second phase, called the positioning phase, uses pattern matching algorithms to match a measurement made by the user's device to the pre-recorded fingerprint database. There are two main classes of algorithms that are used in the positioning phase. Deterministic fingerprinting algorithms such as Nearest Neighbour (NN) calculate the distance in signal space between the measurement and each of the stored fingerprints; the one with the minimum associated distance is assumed to be the location of the user. Probabilistic methods output a likelihood function which gives the probability that the user is located at a specific location. Probabilistic methods are generally more accurate and more complex than deterministic methods. In our system, we use a

technique introduced in [15] and refined in [16] called the Kernel method, which falls in the probabilistic category. The main idea behind that method is that for every access point (AP), the signal strength at a specific location is modelled as a Gaussian distribution centred on the value of the training data, and with an empirically determined standard deviation. The method detailed in [16] also takes into account missing and extra APs which are APs who appear in the training data but not in the user measurement or vice versa. Table 1 details the algorithm used. The probability that the user Wi-Fi measurement  $z_t$  is located at fingerprint  $f_k$  is noted  $w_{total}$ .

The critical part of all fingerprinting positioning systems is the fingerprint database. Indeed, the more data is collected during the training phase the better the wireless environment is known by the system and the higher the final accuracy will be as shown in [17]. However, building such an accurate database requires huge amounts of time and effort and is still the main barrier against further commercial development of indoor positioning systems. A balance needs to be found between the final accuracy that is required and the effort needed to build the database. In our system, the environment is first modelled as a set of nodes and links. Nodes can either represent a physical point of junction between two links or can be used to locate points of interest to the BVI. Links represent typical walking paths inside a building. In most indoor environments, walking patterns are heavily restricted by the floor design. In a typical office building, movement is possible along long corridors or is constrained by furniture such as in an open space office for instance. Therefore, to provide high level navigation, we chose to only map the public parts of indoor environments in opposition to other systems which map every single room of a building. This architecture is very flexible as it allows dropping any point of interest on the links network in order to notify the BVI user of important information. It also provides the positioning engine with additional information on the environment which can be used to do map matching for instance. Moreover, if specialized UI tools were to be developed in order for an operator to enter this information, the time needed to configure the system would be minimal.

TABLE I. WI-FI POSITIONING ALGORITHM

1	$w_{hit} = w_{extra} = w_{miss} = 1$
2	<b>Get APs from measurement <math>z_t</math> and fingerprint <math>f_k</math></b>
3	<b>For all APs <math>h \in Hit</math> do</b> $w_{hit} = w_{hit} \cdot p_{hit}(z_t^h   f_k)$
4	<b>For all APs <math>e \in Extra</math> do</b> $w_{extra} = w_{extra} \cdot p_{extra}(z_t^e   f_k)$
5	<b>For all APs <math>m \in Miss</math> do</b> $w_{miss} = w_{miss} \cdot p_{miss}(z_t^m   f_k)$
6	$w_{total} = \sqrt{ Hit } \cdot w_{hit} \cdot w_{extra} \cdot w_{miss} \cdot \left( \frac{ Hit }{ Hit  +  Extra  +  Miss } \right)$
7	<b>Return <math>w_{total}</math></b>

where

$$\begin{cases} p_{hit}(z_t^h | x_t) = e^{-\frac{(RSSI_{measurement} - RSSI_{fp})^2}{2 \cdot \sigma^2}} \\ p_{extra}(z_t^e | x_t) = e^{-\frac{(PENALTY_{extra})^2}{2 \cdot \sigma^2}} \\ p_{miss}(z_t^m | x_t) = e^{-\frac{(PENALTY_{miss})^2}{2 \cdot \sigma^2}} \end{cases}$$

The penalties  $PENALTY_{extra}$  and  $PENALTY_{miss}$  used in the equation above depend on the signal strength of the missing or extra access point. Indeed, the stronger an access point can be seen the lower the probability that it will not appear in the measurement and vice-versa. More details can be found in [16].

### E. Motion Model

#### 1) Accelerometer, PDR

The accelerometer of the phone outputs data at a rate of 50Hz, giving acceleration values in  $m.s^{-2}$  along the 3 axis attached to the phone's body. The x and y axis are parallel respectively to the width and length of the smartphone's screen and the z axis completes a Cartesian system of axis. In order for the step detection algorithm to work independently of the phone's orientation, we only retain the amplitude of the acceleration:

$$a_k = \sqrt{a_{x_k}^2 + a_{y_k}^2 + a_{z_k}^2} \quad (1.2)$$

We then remove the Earth's gravity from the values by applying a simple high-pass (HP) filter to the acceleration amplitudes. The HP filter follows the following equations:

$$\begin{cases} \mu_k = 0.1 * a_k + 0.9 * \mu_{k-1} \\ a_k^{HP} = a_k - \mu_k \end{cases} \quad (1.3)$$

The resulting signal has a mean of zero and only contains high-frequency components. To reduce the noise of the signal, a low-pass filter is then applied by using a moving average filter. We average 5 samples which correspond to a time period of 100ms. In this way, most of the high-frequency noise is filtered out but the signal retains its low-frequency attributes. A sample of the resulting filtered signal is illustrated in Fig. 3.

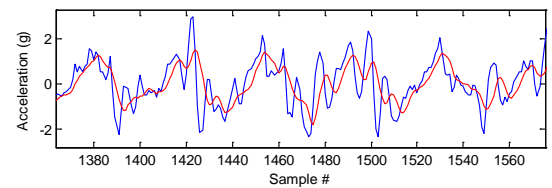


Figure3. In red, acceleration signal after LP and HP filters. In blue, signal after HP filter but before LP filter.

Two operations are then conducted on the filtered signal in order to feed the person's motion model. First, we run a basic test to determine if the person is moving or stationary, similarly to [18]. In order to do so, we compare the acceleration value with an empirically determined fixed threshold. In theory, constant velocity would not be detected by this algorithm. In real life however, movement will always produce accelerations that can be detected (each step produces a peak in the signal for instance). In the algorithm, if the value is above the threshold and stays above it for a number of samples, then movement is detected. If it is below and stays below for a number of samples, the user is assumed to be stationary. In our experiments, the threshold is fixed at  $0.3 \text{ m.s}^{-2}$  and we check the last 5 available samples. In the future, more complex methods will be investigated such as presented in [19]. Those methods have the advantage to recognize more activities such as going upstairs or downstairs, running, etc. However, they are more computationally intensive and we will determine if they can be implemented on a smartphone.

The next operation is to estimate the speed of the user. In order to do so, a step detection algorithm coupled with a step size model is used. Most step detection algorithms assume the user is holding the device is located in a specific location on the user's body such as in the pocket ([18]) or on a foot where the measured accelerations are the most clear to detect steps and the Zero Velocity Update (ZUPT) algorithm can be applied such as in [20]. However, as explained in section II.A, one cannot require a BVI person to hold the phone in any particular position. Thus, we exploit the fundamental periodicities in the acceleration signal to detect the step frequency of the user. Indeed, walking is a periodical activity at its core and its main period is determined by the step frequency. In order to investigate this idea, a simple experiment was conducted where a user carries the phone in his hand and walks at a relatively constant step frequency for a period of time. A Fast Fourier Transform (FFT) was then executed on the whole filtered acceleration signal. The output is presented in Fig. 4. A sharp peak can be observed at a frequency of 1.36 Hz which is very close to the actual recorded step frequency of 1.34 Hz. A

similar test was run where the phone was placed in one of the lateral trousers pocket. Once again a sharp peak was detected with a frequency of 1.51Hz where the real step frequency was 1.43Hz.

The sampling rate of the smartphone accelerometer can be adjusted for different uses. In our experiments, we chose a sampling rate of 10Hz which results in a maximum step frequency detectable of 5 Hz, high enough unless the user is sprinting down a corridor. The length of the window on which the FFT is applied is a critical parameter. It determines the resolution in time and frequency domain. If too long, the resolution in the time domain is too small, i.e. different speeds at different times cannot be separated. For instance, if the FFT is applied on a 10 seconds window, it will result in only one speed value whereas the speed of the user could have changed dramatically within these 10 seconds. If the window is too short, the resolution in frequency domain is too high, i.e. close walking frequencies cannot be separated. This results in a lack of accuracy in the speed measurement. We chose a window size of 2 seconds (20 samples). The samples are then padded with trailing zeros so that the FFT is executed on 1024 points. The FFT is run on a sliding window which moves every 5 samples, which gives us a step frequency value twice per second.

Once the step frequency has been estimated, the step size is still needed in order to compute the estimated speed of the user. In our context, the step size is defined as the distance from the heel of one foot to the heel of the other foot. In [10] and [21], the step size is assumed to increase linearly with the step frequency following this model. However, the step size is not only a function of step frequency but also depends on the height of the user. In [18], the step size is modelled as a linear function of the height  $l_s = k * h$  where  $k$  only depends on the sex of the user. In our model,  $k$  varies linearly with the step frequency following this model:

$$\begin{cases} l_s = (a + b \cdot f_s + \varepsilon) * h \\ \varepsilon \sim N(0, \sigma_s) \end{cases}$$

The parameters of the model  $(a, b, \sigma_s)$  are estimated from empirical data. The results are detailed in part III.A.

## 2) Compass

For the motion model to be complete, a heading value of the user's movement must be obtained. This is challenging first because the user's heading might be different from where he is headed. In the case of a BVI person, he/she might be "scanning" with his/her long cane while moving in one direction. Or the phone could be placed in the pocket or backpack of the user, making it very hard to determine a value from the magnetic field sensor. In our experiment, we assume that the user will be holding the phone in his/her hand, with the screen facing upwards and the top of the phone facing forward. However, this is clearly not practical for the BVI as discussed in part II.A. A solution would be to design and build a small magnetic sensor that can be pinned on the chest or integrated in the cane. The sensor can then send all the data to the phone

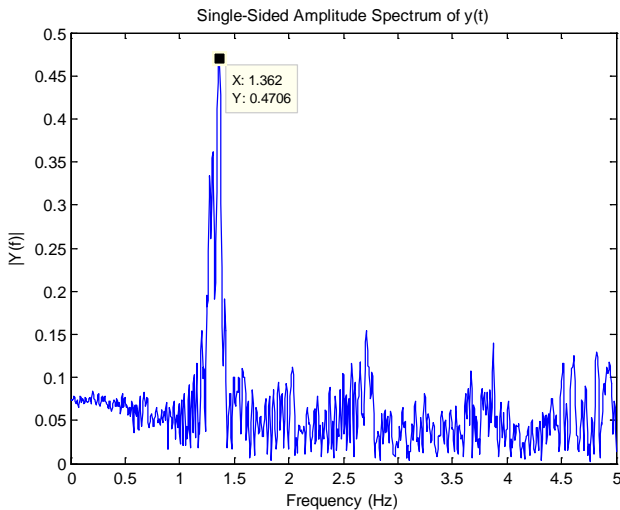


Figure 4. Initial test for step frequency estimation using FFT

using a low power Bluetooth data link. An example of such a device can be found in [22].

To increase the accuracy of the heading, two methods are possible. The first is to fuse rotation information from other available sensors, gyroscopes for instance. Although gyroscopes do not provide an absolute heading value and are quite noisy, they can be used to identify when the user is turning and are not subject to interference from metal objects. They can therefore be used to filter out big heading changes that occur because of indoor metal structures. Another simpler technique that can be used is “heading matching”. Map matching is a technique used for car navigation outdoors and that leverages on the simple knowledge that a car is bound to be on a road, and thus any GPS position that is not located on a road is wrong. Indoors, although no roads are available, the environment and possible movements of the user are generally quite constrained. In a typical office building, public areas are generally organised as corridors, small lobbies, etc. In a corridor for instance, only two heading values are possible when the user is walking. Thus, with the knowledge of the building’s layout, it is in theory possible to filter out headings coming from the magnetic sensor. This technique has not been implemented yet.

#### F. Map matching

In order to increase the accuracy of the system, knowledge of the building layout is as important as the positioning technology itself. As our system is only designed to provide position and navigation in public areas of a building, a simple map matching technique has been implemented which forces the calculated position to stay in those areas. If the position drifts outside, it is simply projected back to the closest position in a public area. Of course, more complex map matching techniques exist and will be investigated in the future.

### III. TESTS AND TUNING

#### A. PDR tests

##### 1) Step frequency estimation

In order to test the accuracy of the step frequency estimation algorithm, data was collected as follows. Four users, two males and two females were asked to walk along a corridor holding the phone in their hand with the top of the screen facing forward. Each user was then asked to walk at constant speed (and therefore constant step frequency), holding the phone as they would do normally. Each user did four walks along the corridor, resulting in 16 data sets. Of these 4 walks, each user was asked to do one at a very slow (unnatural) speed, two at a “normal” speed for them, and one at a very high (unnatural) speed. In order to estimate the step frequency, the FFT was run on a 2 second window and a simple peak detection algorithm was run to find the step frequency (see section II). Fig 5 shows the mean error of the step frequency estimation related to the real step frequency. As can be seen, the algorithm works very well at natural and high speeds. Indeed, when walking at these speeds, the acceleration signal is “cleaner” and peaks appear more clearly. Therefore, the FFT is able to detect periods in the signal more efficiently. The problem lies in very low step frequencies (less than 1.4 Hz)

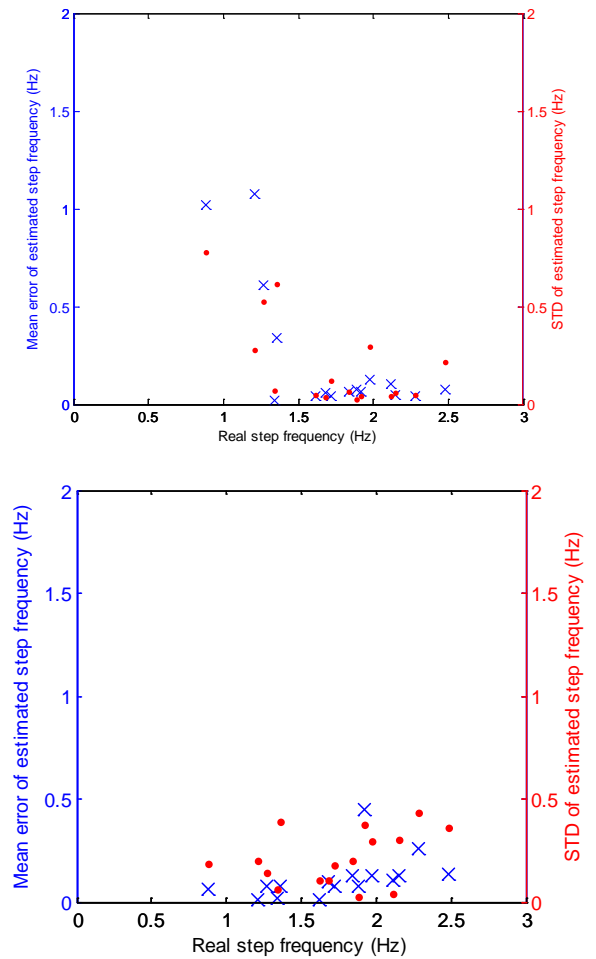


Figure 5. Step frequency estimation, initial and updated results

where the accuracy of the estimation is degraded. The standard deviation of the frequency estimation was also computed and once again, it is lower at normal and higher walking speeds and degraded at slower walking speeds.

In order to solve this problem, it was observed that at low step frequencies, the spectrum of the signal was a lot “flatter” and the amplitude of the peaks in the FFT much smaller. This was observed for all of the four users, and at comparable levels. A simple threshold algorithm was added to the peak detection algorithm to detect those conditions that limits the search for the peak in the lower step frequencies interval, below 1.4 Hz in our case. Fig. 5 shows the updated results. As can be seen, the accuracy of the step frequency estimation has increased a lot in the lower frequency range, and the performance of the algorithm is very satisfactory. Ignoring one outlier, the algorithm manages to estimate the step frequency with an average accuracy 0.11 Hz, a maximum error for one walk of 0.4Hz. The average standard deviation for all runs is 0.21Hz and the maximum standard deviation is roughly 0.4Hz.

Now that the step frequency is estimated with a relatively good accuracy, the step size still needs to be determined in order to compute a speed value for the motion model.

## 2) Step size estimation

In order to estimate the parameters of the step size model described in part II.E, experimental data was collected using the phone's in-built accelerometer. Four participants were asked to hold the phone in their right hand and walk for a given distance (36 meters). The four participants have heights that range from 167cm to 196cm, two women and two men, and were asked to try as much as possible to maintain a constant speed during the test. At the same time, their walk was recorded on video and the step number of each run was later calculated. Each participant did four runs and was asked to vary his/her walking speed from very slow to very rapid. For the experiment, we assumed constant step frequency and constant step size. Fig. 6 shows the scatter plot of the  $(l_s / h, f_s)$  pairs which should follow a linear relationship as detailed in part II.E.

As can be seen, the data fits quite well to the model and the calculated model parameters that will be used in the speed estimation algorithm are:

$$(a, b, \sigma_s) = (0.15, 0.14, 0.044)$$

These parameters are used for the initial implementation of the system but should be refined by gathering data from more participants.

## B. Compass test

The compass on the phone was tested in an indoor environment. Two main characteristics of the compass were tested. The first is of course the accuracy of the heading value. The second is the time drift in order to evaluate if the error is consistent or time dependant. The test procedure was the following. Four cardinal directions were tested in our building. For each complimentary pair of headings, the phone compass was calibrated once by following the procedure described in the phone's manual and then the operator walked back and forth along the corridor 5 times. The corridors were roughly 40 meters long, for a total walking time of 6 minutes. The reference headings were obtained through Google Earth and the magnetic declination in Sydney was calculated using [23]. Table 2 summarizes the results.

As can be seen, large heading errors can be observed mainly due to the amount of metal contained in the building structure and rooms. However, it is interesting to note that even in the case of the maximum error observed (about 60 degrees), it is possible to know in which direction the user is heading

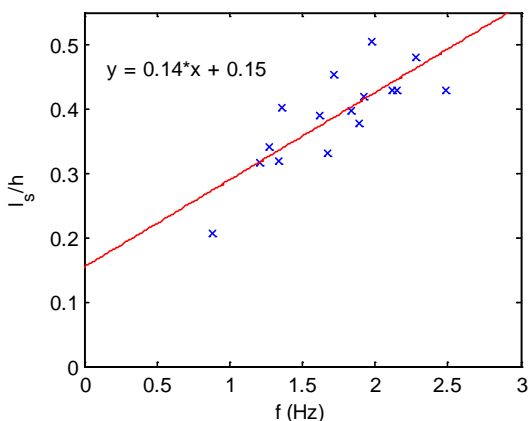


Figure 6. Step size model parameters estimation

along a corridor. Thus, it is possible in theory to use the heading-matching technique described in part II.E.

TABLE II. COMPASS ERROR CHARACTERISTICS

<b>True heading (deg)</b>	8	98	188	278
<b>Average error (deg)</b>	13	13	13	11
<b>Standard deviation (deg)</b>	10	13	12	13
<b>0.95 confidence interval (deg)</b>	30	33	32	28
<b>Max error (deg)</b>	52	58	54	57

Another important observation is that all the values observed are very similar for the four cardinal directions. This suggests that the performance of the compass does not vary with time as the four tests were done at different times. Reference [24] also finds out the same results. Fig. 7 displays the heading value computed by the compass for three of the four tests and showing the five runs along the corridor. It can be observed that the variation of the heading is quite similar from one run to another, suggesting that the compass performance depends more or less solely on the magnetic characteristics of the building rather than on time or other factors.

## C. Final accuracy tests

In this part, we present the final accuracy tests of our system, and tune the noise covariance matrixes  $Q$  and  $R$  of the Kalman filter to obtain optimal performance. Data was gathered as follows. First the Wi-Fi fingerprints database was built. The experiment took place on Level 4 of the Electrical Engineering building at the University of New South Wales, Sydney. The level has a surface of approximately 3000 square meters. In the public areas of the level, 270 fingerprints were collected along the "rails" described in section II part B. All the fingerprints were collected in less than 10 minutes. A more detailed survey will of course increase the accuracy of the positioning, but our goal is to prove that a practical accurate positioning system is possible. Then, three people, with heights ranging from 175cm to 195cm, were asked to walk along a predefined path three times at varying speeds. Before each run, the magnetic sensor was calibrated using the manufacturer's recommended procedure. In order to obtain ground truth, start

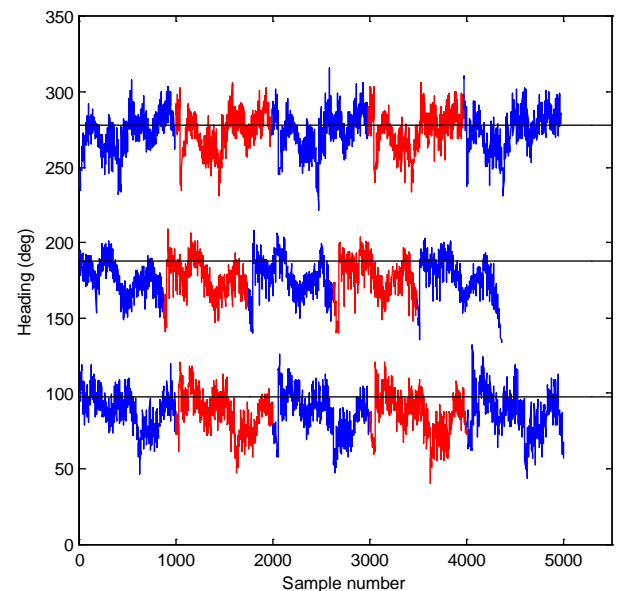


Figure 7. Heading value repeatability over time

and end times were recorded and the user was asked to walk at constant speed as much as possible. Our method was compared with the well-known Nearest Neighbour algorithm and the Kernel method described in section II, part D.

As detailed previously, the choices of matrixes  $Q$  and  $R$  are crucial for the performance of the Kalman filter. Therefore for each test, the average accuracy and standard deviation of the position were computed for several matrixes. The matrixes were of the form  $Q = q * I$  and  $R = r * I$  as there is no reason to apply different noise values to the x and y coordinates. A look up table was built and a total of 256 combinations of  $(q, r)$  combinations were tested. Intuitively,  $Q$  and  $R$  represent the amount of noise and the trust that one can have in the motion model and in the Wi-Fi positions respectively. Therefore, increasing or decreasing  $q$  and  $r$  together will have very little effect on the filter's behaviour. It is more the relationship between  $q$  and  $r$  that is relevant. Fig. 8 confirms this intuition. It shows the average accuracy against the different  $q/r$  ratios tested. As can be seen, there is an ideal ratio  $q/r$  that minimizes the resulting accuracy of the filter.

Table 3 details the results of the tests performed for all users. As can be seen, the filter performs very well with an average increase of accuracy of almost 1.8 meters, corresponding to a 37.5% increase compared to the Kernel method. Compared to the NN algorithm, the Kalman filter is 2.8 meters more accurate on average, corresponding to a 50% increase. The problem lies in the choice of the  $q/r$  ratio. The optimal ratio varies greatly between users and even between different tests for the same user. This is mainly due to the unpredictability and great variability of the Wi-Fi measurements. The motion model's performance is much more stable than the Wi-Fi positioning engine and thus, the authors believe that the greatest challenge lies in the choice of the  $R$  matrix. This problem is of course closely linked to error estimation of Wi-Fi fingerprinting systems, which is still a vast field of research. However, it needs to be addressed before any practical implementation of the filter can be made.

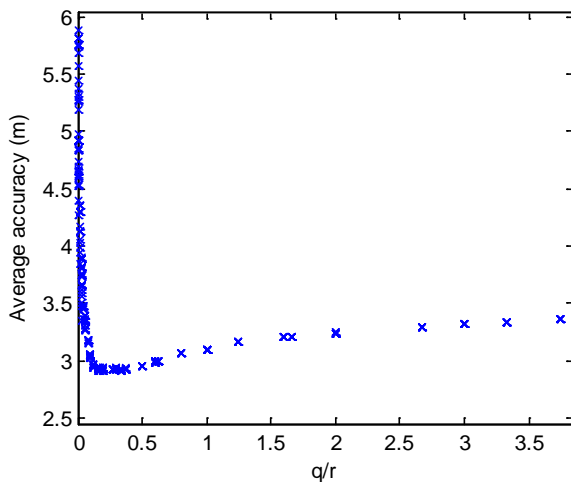


Figure 8. Impact of the  $q/r$  ratio on accuracy for a particular user/ experiment

TABLE III. DETAILS OF TESTS OF KALMAN FILTER ACCURACY

Test	NN Average (m)	Kernel Average (m)	Kalman Average (m)	Kalman Std (m)	q/r
User1	4.67	3.69	2.91	3.33	0.17
User1	3.95	3.44	2.91	2.67	0.2
User1	4.95	3.48	2.41	1.73	0.08
User2	5.57	3.87	2.57	1.7	0.01
User2	7.07	5.3	2.43	1.7	0.006
User2	7.1	6.87	4.12	3.35	0.00625
User3	5.82	5.03	3.44	2.13	0.0625
User3	6.61	5.54	3.65	3.04	0.0125
User3	6.47	6.08	3.28	1.79	0.0027

#### D. Initial implementation

Fig. 9 shows an initial implementation of the system on a Galaxy Nexus smartphone running Android. All the algorithms run in real time on the phone and a new position is delivered by the filter every 700ms.

#### IV. CONCLUSION

In this paper, we first examined in detail the user requirements of the BVI for an indoor and outdoor positioning system. The usability and robustness of the system have been shown to be as important as the accuracy. Indeed, obstacle avoidance is a task that is already solved by primary navigation aids such as the long cane, or guide dog. The authors believe that these solutions cannot be beaten by technology, at least not



Figure 9. Early implementation of the system on an Android smartphone



in its current state. They can however, be augmented with technologies such as ultrasound for instance. But what the BVI lack most is signage and high-level information about their environment. This is what GPS and other positioning technologies, and the Location Based Services that leverage them, have brought to sighted people, and this is what needs to be made accessible to the BVI and to handicapped people more broadly.

As part of this effort, an indoor positioning system that runs on a mid-range smartphone has been developed. It relies at its core on a Kalman filter that fuses the information delivered by all the sensors embedded on the phone. In our tests, the system managed a 35% increase compared to the most advanced Wi-Fi only algorithm, and a 50% increase to the classical NN algorithm. This is accurate enough to deliver the signage and contextual information to the BVI. However, there are still issues that need to be addressed before practical implementation can take place, especially with the choice of the noise covariance matrixes of the Kalman filter.

Future research will focus on addressing these issues and on designing the interface to deliver the information to the BVI in an accessible and efficient way.

#### ACKNOWLEDGEMENTS

This work has been funded by the Australian Research Council linkage grant number LP0989176.

#### REFERENCES

- [1] (2012, Jul.). A new frontier for Google Maps: mapping the indoors [Online]. Available: <http://googleblog.blogspot.fr/2011/11/new-frontier-for-google-maps-mapping.html>
- [2] E. Wise, E. Ramsey-Stewart, B. Li, T. Gallagher, A.G. Dempster, C. Rizos, D. Woo, "Indoor Navigation for the Blind and Vision Impaired: Where are we and where are we going?", submitted to International conference on Indoor Positioning and Indoor Navigation (IPIN2012), 13-15 November 2012.
- [3] E. M. Ball, "Electronic Travel Aids: An Assessment," in *Assistive Technology for Visually Impaired and Blind People*, M. A. Hersh and M. A. Johnson, Springer London, pp. 289-321.
- [4] B. Hoyle and D. Waters, "Mobility AT: The Batcane (UltraCane)," in *Assistive Technology for Visually Impaired and Blind People*, M. A. Hersh and M. A. Johnson, Springer London, pp. 209-229.
- [5] M. Wood, "Trekker Breeze 2.0: Trialled by Clients," in *International Journal of Orientation and Mobility*, vol. 1, num 1, 2011, pp. 78-83.
- [6] B. Li, E. Ramsey-Stewart, K. Johar, D. Woo, C. Rizos, "More freedom to the Blind and Vision Impaired – A Proposed Navigation and Information System", IGNS Symposium 2009, Gold coast, Australia, 1-3 December, 2009.
- [7] Y. Li, A. Tsai, P. Mumford, W. Lin and I. Hong, "Continuous high precision navigation using MEMS inertial sensors aided by RTK GPS for mobile mapping applications", *Coordinates*, VII(2), 2011, February, 7-12.
- [8] D. Gusenbauer, C. Isert, and J. Krösche, "Self-contained indoor positioning on off-the-shelf mobile devices," in 2010 International Conference on Indoor Positioning and Indoor Navigation (IPIN), 2010, pp. 1–9.
- [9] Q. Ladetom "Capteurs et algorithmes pour la localisation autonome en mode pédestre", PhD Thesis, École Polytechnique Fédérale de Lausanne (EPFL), Lausanne, Publ. No. 2710, 2003, pp. 60-64.
- [10] H. Lemelson, M. B. Kjærgaard, R. Hansen, and T. King, "Error Estimation for Indoor 802.11 Location Fingerprinting," in *Proceedings of the 4th International Symposium on Location and Context Awareness*, Berlin, Heidelberg, 2009, pp. 138–155.
- [11] P. Myllymaki et al., "Error estimation concerning a target device's location operable to move in a wireless environment", US patent 7,209,752B2, 24 April 2007.
- [12] V. Moghtadaiee, and A.G. Dempster, "WiFi Fingerprinting Signal Strength Error Modeling for Short Distances", submitted to International conference on Indoor Positioning and Indoor Navigation (IPIN2012), 13-15 November 2012.
- [13] P. Bahl and V. N. Padmanabhan, "RADAR: An in-building RF-based user location and tracking system," in *INFOCOM 2000. Nineteenth Annual Joint Conference of the IEEE Computer and Communications Societies. Proceedings. IEEE*, 2000, vol. 2, pp. 775–784.
- [14] T. Gallagher, B. Li, A.G. Dempster, and C. Rizos, "A sector-based campus-wide indoor positioning system", *Indoor Positioning and Indoor Navigation conference (IPIN)*, pp. 1-8, 15-17 September 2010.
- [15] T. Roos, P. Myllymäki, H. Tirri, P. Misikangas, and J. Sievänen, "A Probabilistic Approach to WLAN User Location Estimation," *International Journal of Wireless Information Networks*, vol. 9, no. 3, pp. 155–164, Jul. 2002.
- [16] M. Weyn, "Opportunistic Seamless Localization," PhD, Universiteit Antwerpen, 2011, pp. 58-64.
- [17] B. Li, J. Salter, A. G. Dempster, C. Rizos, and others, "Indoor positioning techniques based on wireless LAN," in *First IEEE International Conference on Wireless Broadband and Ultra Wideband Communications*, Sydney, Australia, 2006, pp. 13–16.
- [18] I. Bylemans, M. Weyn, and M. Klepal, "Mobile Phone-Based Displacement Estimation for Opportunistic Localisation Systems," in *Mobile Ubiquitous Computing, Systems, Services and Technologies, 2009. UBIComm '09. Third International Conference on*, 2009, pp. 113 –118.
- [19] A. M. Khan, Y.-K. Lee, S. Y. Lee, and T.-S. Kim, "Human Activity Recognition via an Accelerometer-Enabled-Smartphone Using Kernel Discriminant Analysis," 2010, pp. 1 –6.
- [20] Widyawan, M. Klepal, and S. Beaugard, "A Backtracking Particle Filter for Fusing Building Plans with PDR Displacement Estimates", *WPNC*, Hannover, Germany, March 2008.
- [21] R.W. Levi, T. Judd, "Dead Reckoning Navigational System Using Accelerometer to Measure Foot Impacts," U.S. Patent Number 5,583,776, 1996.
- [22] J. Chung, M. Donahoe, C. Schmandt, I.J. Kim, P. Razavai, and M. Wiseman, "Indoor location sensing using geo-magnetism," in *Proceedings of the 9th international conference on Mobile systems, applications, and services (MobiSys '11)*, 2011.
- [23] (2012, Jul.). NOAA's Geophysical Data Center - Geomagnetic Data [Online]. Available: <http://www.ngdc.noaa.gov/geomagmodels/struts/calcDeclination>
- [24] B. Li, T. Gallagher, A.G. Dempster, and C. Rizos, "How feasible is the use of magnetic field alone for indoor positioning?", submitted to International conference on Indoor Positioning and Indoor Navigation (IPIN2012), 13-15 November 2012.